Stanford Exploration Project, Report 70, December 18, 1997, pages 1–145

Stanford Exploration Project, Report 70, December 18, 1997, pages 1–145

Prestack reverse-time migration in anisotropic media

Martin Karrenbach[1]

keywords: *amplitudes, anisotropy, modeling, algorithm, imaging, elastic*

ABSTRACT

The finite-difference method used with the full two-way wave equation can model all wave phenomena exhaustively and provides correct amplitude information at reflectors. Reverse time migration, or conjugate-gradient inversion, uses conjugate modeling to arrive at an approximate inverse to the forward modeling process. Reverse time migration is expensive compared to one-way wave equations or algorithms with simplified reflection geometry, but it handles all amplitudes properly and includes all wave propagation phenomena. Reverse time migration is suggested as the preferred tool for detailed medium property identification.I show a two-dimensional example, where elastic siffnesses in an anisotropic media can be imaged and determined by crosscorrelating strain components of a forward-modeled shot wave field with strain components of the backward-propagated data wavefield.

INTRODUCTION

In 1988 John Etgen described in detail a staggered-grid finite-difference scheme for arbitrary anisotropic media. He showed forward modeling examples in the plane of symmetry for transverse isotropic (TI) media. He also showed a reverse-time migration image using SH waves. In this paper I will use his staggered-grid method and implement a general anisotropic imaging condition. The possibilities are abundant for implementing imaging conditions for reverse time migrations. These approaches differ in how the forward-modeled shot is handled in the migration step. The use of one-way wave equations or ray-tracing methods leads to fast algorithms, but such short cuts also give incorrect amplitude information. The development of the imaging condition for arbitrary anisotropic media used in this paper follows Peter Mora's description (1989) of the conjugate elastic wave-equation operator. He showed the relationship between the imaging condition and conjugate-gradient computation. When the right

[1]**email:** not available

imaging condition is chosen, prestack migration becomes one step in the conjugate-gradient iteration.

FORWARD MODELING

The equation for general anisotropic elastic wave propagation is

$$\partial_j \; c_{ijkl} \; \partial_l \; u_k = \rho \; \partial_{tt} \; u_i - f_i, \tag{1}$$

where c_{ijkl} is the elastic stiffness tensor, ρ the density, f_i the source function, and u the displacement field.

Transverse isotropy is the next more complex symmetry class after isotropy. It allows the description of material properties like those of shale or layered isotropic mixtures (Muir 1990).

In approaching the anisotropic forward propagation problem I followed Etgen: I used the explicit finite-difference stress-strain formulation to solve the anisotropic wave equation. Since the time step size is limited by a stability criterion, this method is somewhat more expensive than methods using one way equations. On the other hand, within the stability limit accurate amplitudes are obtained in the computed wavefield, without any dip limitation. An additional advantage is material parameters that are freely variable in space.

Recent processing techniques tend to emphasize preservation of amplitude information during all processing steps. When not only imaging subsurface structure, but also determination material properties is important, algorithms based on two-way equations are the best way to ensure correct amplitudes and allow for full complexity of the wavefield. Algorithms based on the one-way equation will necessarily give incorrect reflection amplitude information.

THE CONJUGATE

Peter Mora (1986) showed the conjugate operation to the elastic forward modeling and used it to find iteratively the inverse of elastic wave propagation. With his notation, the solution for perturbations to wave equation (1) can formally be written in terms of Green's functions:

$$\delta \; u_i = \int_V G_{ij} * \delta \; f_j \; - \int_V \partial_t \; G_{ij} * \partial_t \; u_j - \int_V (\partial_k \; G_{ij}) * (\delta \; c_{jklm} \; \partial_m \; u_l) \delta \; u_i. \tag{2}$$

When ignoring perturbations in the source function or in density, the adjoint (transpose) can be written in terms of material parameters:

$$\delta \; c_{jklm} \;\; = \;\; - \int \; dt \; \partial_k \; G_{ij} * \partial_m \; u_l \; \delta \; u_i. \tag{3}$$

The above equation is intuitively more understandable when written in terms of wavefields:

$$\delta\ c_{jklm} \ = \ \int\ dt\ [\partial_m\ u_l(x,t)]\ [\partial_k\ \delta\ \psi_j(x,t)], \tag{4}$$

where u is the forward-propagated shot wavefield and ψ is the backward-propagated data (in the case of prestack migration) or the residual data (in the case of Mora's inversion).

Changes in the material parameters can be estimated by crosscorrelating the backward-propagated modeled strain field and the backward-propagated data strain field. Both fields are tensor fields and what are crosscorrelated are actually the strain tensor components. In terms of prestack migration this crosscorrelation is the imaging condition. In the following I use this imaging condition to find perturbations of elastic stiffness parameters for a given starting model. One might ask: why image stiffnesses and not velocities? For isotropic media the imaging of velocities or wave potential works well, because the wave types are separable into a P wave and S wave potential and those potentials are decoupled. In the case of anisotropic media such a decoupling is only possible in a few rare cases of special symmetry. Imaging stiffness naturally evolves out of the anisotropic wave equation and wave types don't have to be decoupled in order to perform imaging. Some stiffness components, however, may not be be very well resolved, depending strongly on the acquisition geometry and source radiation pattern illuminating the subsurface. The above stated imaging condition reduces to the well-known U/D principle (Claerbout, 1986) in the case of an isotropic scalar wavefield.

SYNTHETIC EXAMPLE WITH TRANSVERSE ISOTROPY

For testing the algorithm I used a 2D model consisting of horizontal layers with a vertical discontinuity. Individual layers are made up of isotropic and transverse isotropic materials. The top layer is isotropic, the second one is transverse isotropic (TI), followed by another isotropic/TI sequence. All of them have constant density. I chose horizontal layers to see if the reverse-time migration really could recover relative amplitudes properly along the horizontal direction, and to see how well an image of the fault could be obtained.

A surface spread of 8 km is covered by geophones with 40 m spacing. I used only 16 sources in 400 m intervals at the surface. Choosing a relatively small number of source I wanted to push the method to its limits. Figure **??** shows shot gathers for vertical and **??** horizontal sources, situated at 4 locations along the profile. The triplicating reflected event generated by the TI layer is visible after about 1 s traveltime. Reverse time migrating those 16 shot gathers, the subsurface image is recovered as shown in Figure **??** and **??**. The result is a bandlimited image of the variations in subsurface stiffnesses. The amplitudes correspond to changes in stiffnesses (since I use the backpropagated data wavefield and not the residual wavefield). In general it is the gradient of the material parameters, with which an update of the input stiffness model is possible.

The plane reflectors and the step function are recovered well for C_{33} and C_{44} while C_{11} and C_{13} are recovered less well. Particularly the image of the sources interferes with the image of the reflector and in the upper part of the image. It is a consequence of not removing the first arrival in the shot gathers before migrating. The direct wave energy is then placed at the source position. A combination of dip filter and polarization filter could be used to get efficiently attenuate such energy. In these examples the influence of that energy and the influence of the source radiation pattern is clearly visible in amplitude variations on top of the first reflector. By using only 16 sources the subsurface is not illuminated uniformly and the radiation pattern of the vertical source radiates P energy mainly in the vertical direction, while S energy is radiated off to the sides (non-free surface condition).

For the second reflector the direct wave energy does not interfere much anymore and the curvature of the incident wavefield is rather small, thus a more uniform image is obtained.

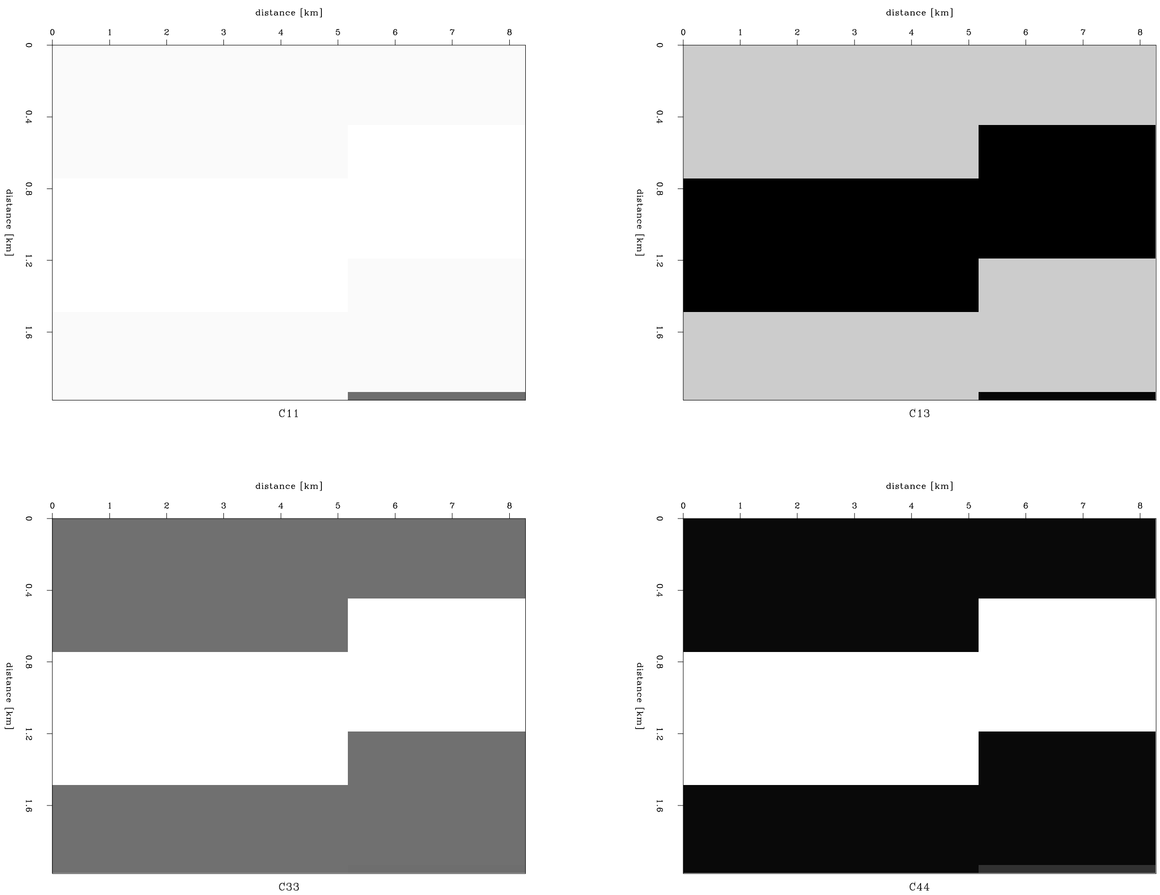

Figure 1: A 2D subsurface model with variable elastic stiffnesses and constant density. martin3-step [NR]

PRACTICAL ISSUES FOR THE CONNECTION MACHINE

The above outlined algorithm is implemented on the Connection Machine. Finite-differences algorithms are very well suited to massively parallel computers, since the computational grid exactly maps onto the layout of processors. I found that my code ran at about 113 Mflops on a 4K machine. The algorithm could be much faster, if it were not for the boundary conditions, which are used to prevent reflections from the side and bottom boundaries. Using a one-way wave equation with absorbing boundaries necessitates the use of different finite-difference stencils in the interior and at various locations at the boundary. If the memory of the machine is big enough, an

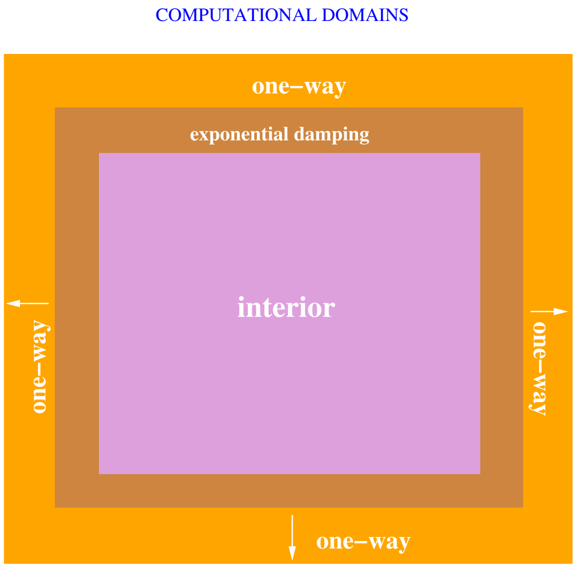

Figure 2: The computational domain in this implementation is divided into three parts: interior, exponential-damping boundary and one-way wave equation absorbing boundaries. In each of those domains different finite difference operators can vary in form domain to domain. An elegant solution is to have a super-stencil, so that the same stencil can be used in all domains. This implies some computational overhead and increased memory use. martin3-domains [NR]

efficient implementation is possible, where spatially variable finite-difference coefficients are used. The shape of the stencil is constant over the entire grid. Using the SEP machine, which has small memory, I could not apply this elegant approach efficiently, since I would have had to truncate my problem size unrealistically. I really liked to use the Connection Machine as a movie program, seeing wave propagation snapshots as they are calculated. This instant feedback makes the machine useful as a teaching tool.

CONCLUSIONS

Elastic stiffnesses in anisotropic media can be determined by crosscorrelating the strain components of a forward-modeled shot wavefield with strain components of the backward-propagated data wavefield. This serves as an imaging condition in the case of prestack reverse time migration. Compared to one-way algorithms, such an implementation is more expensive, but provides correct amplitudes for all events

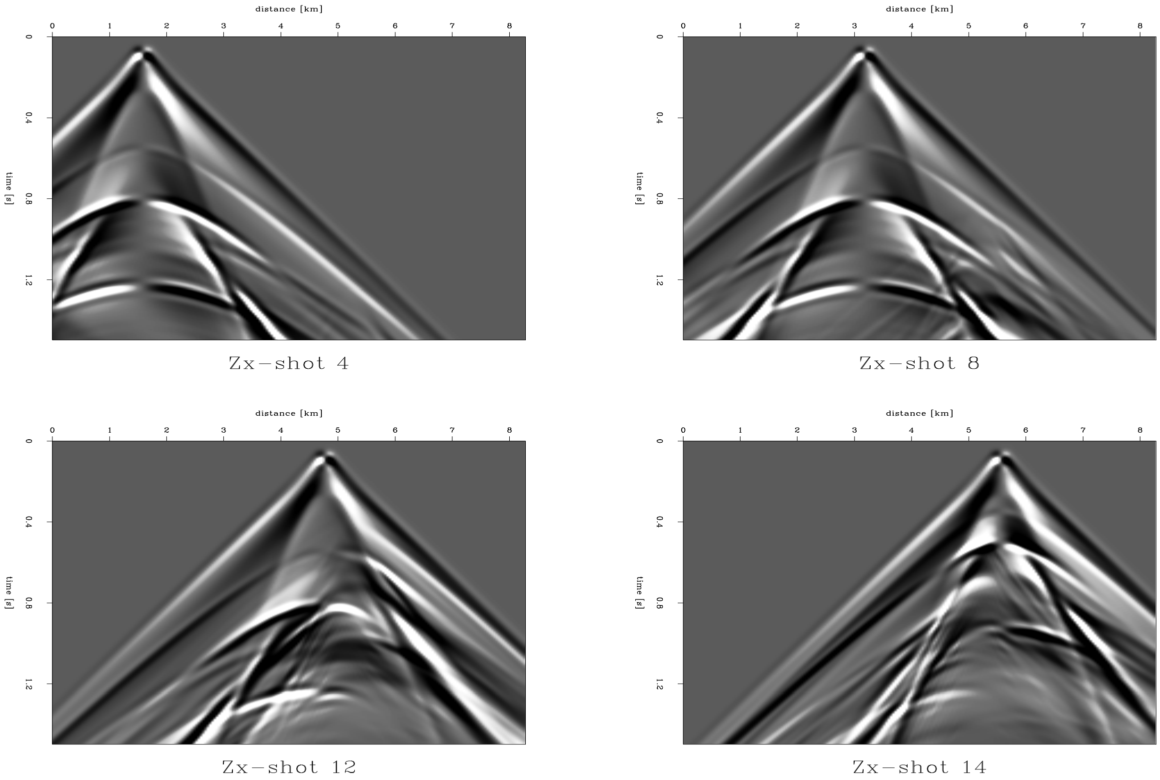

Figure 3: Shot gather generated by a vertical source and horizontal inline receiver. martin3-Zxseis [NR]

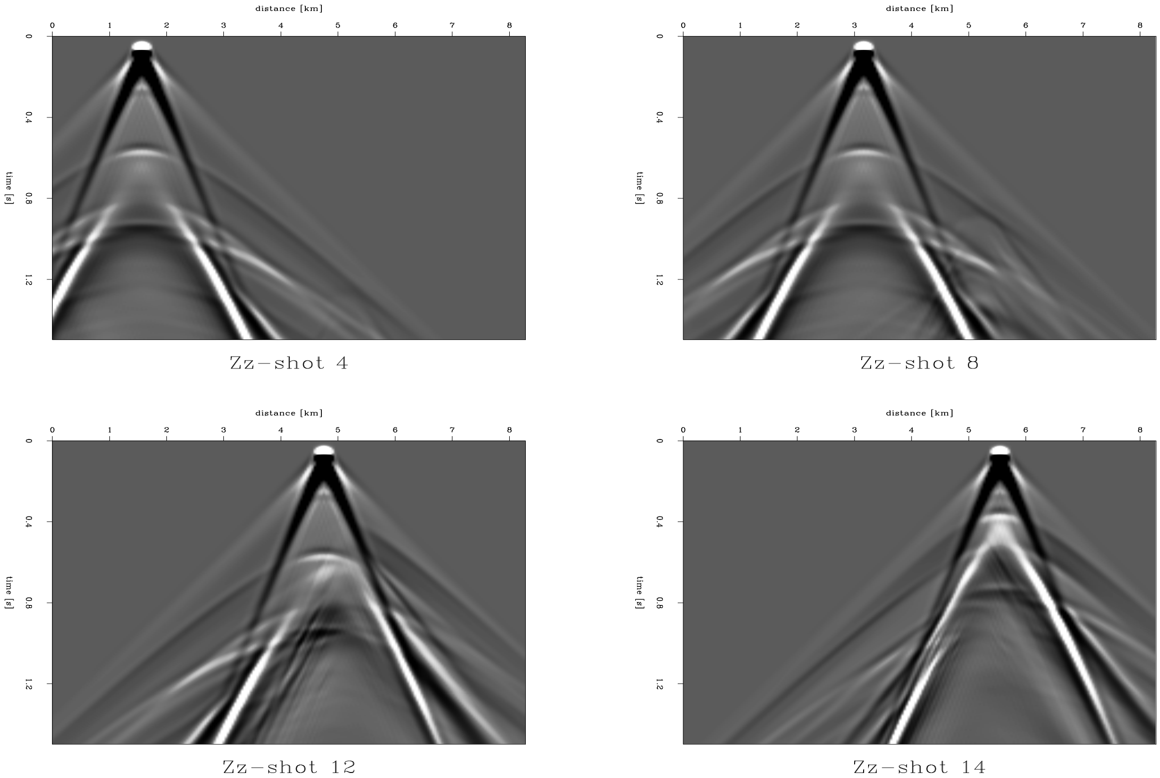

Figure 4: Shot gather generated by a vertical source and vertical receiver. martin3-Zzseis [NR]

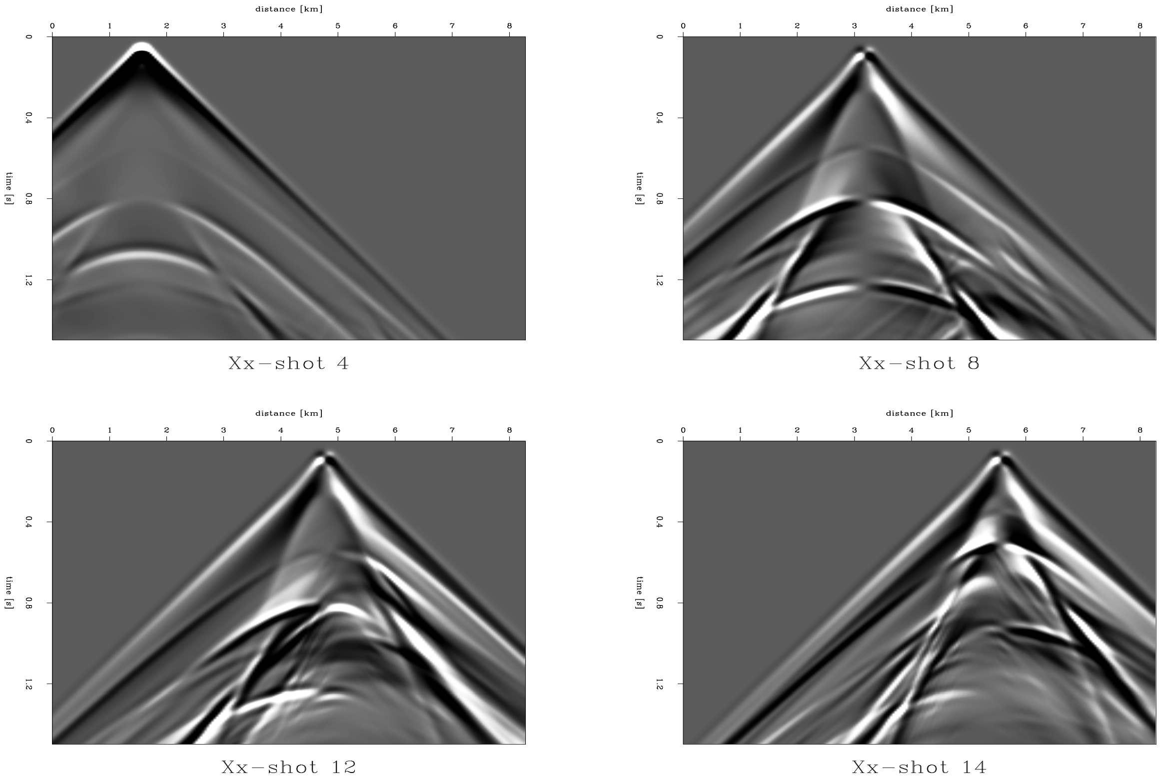

Figure 5: Shot gather generated by a horizontal inline source and a horizontal inline receiver. $\boxed{\text{martin3-Xxseis}}$ [NR]

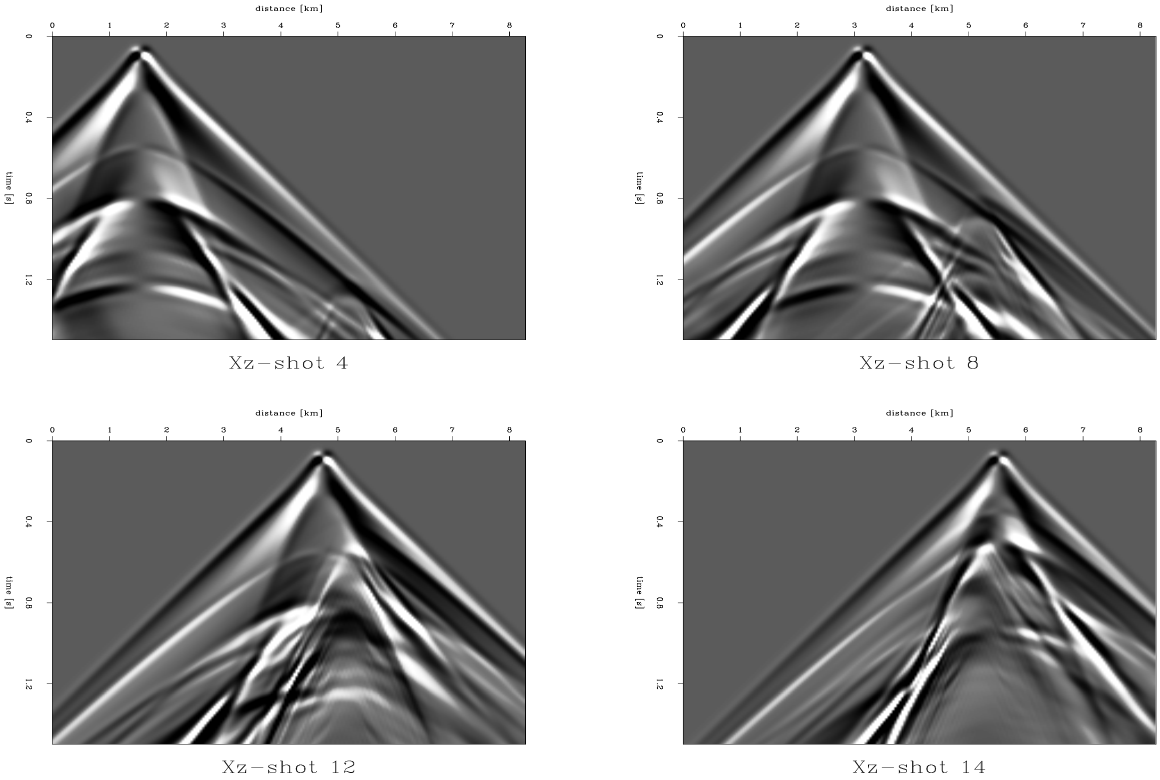

Figure 6: Shot gather generated by a horizontal inline source and a vertical receiver. martin3-Xzseis [NR]

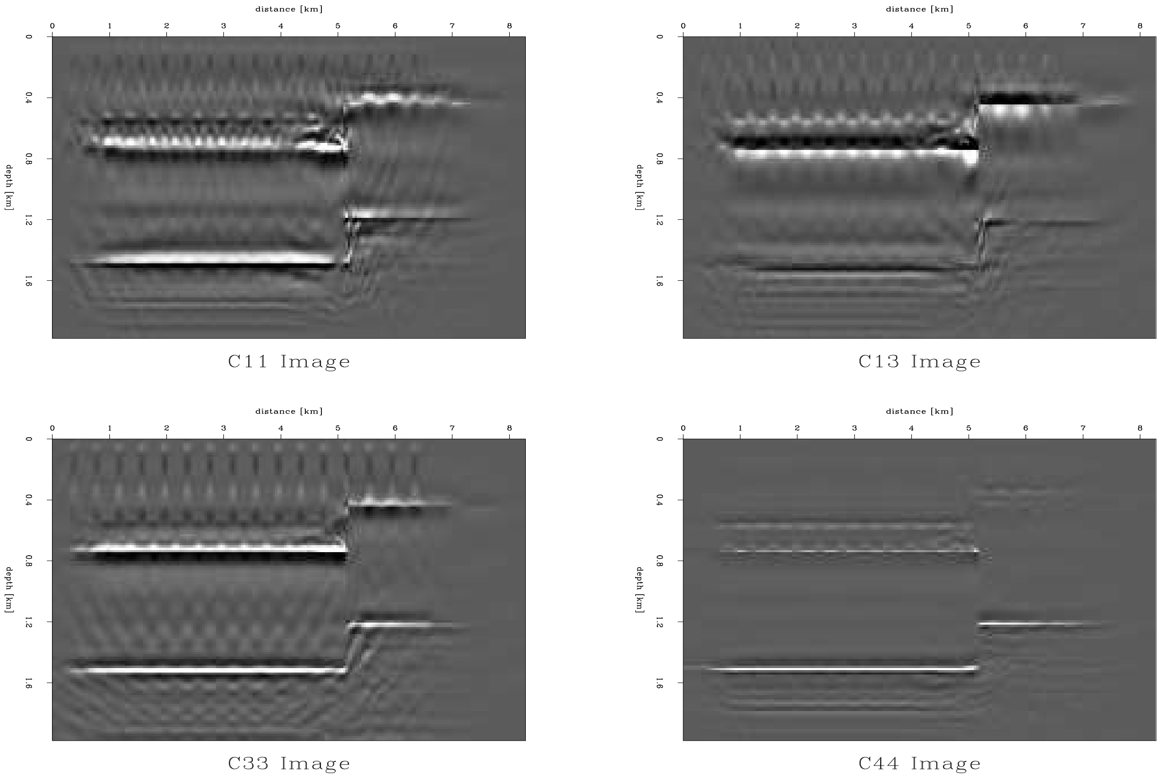

Figure 7: Elastic stiffnesses imaged using 16 shots. Source vector was vertical. martin3-zimagestack [NR]

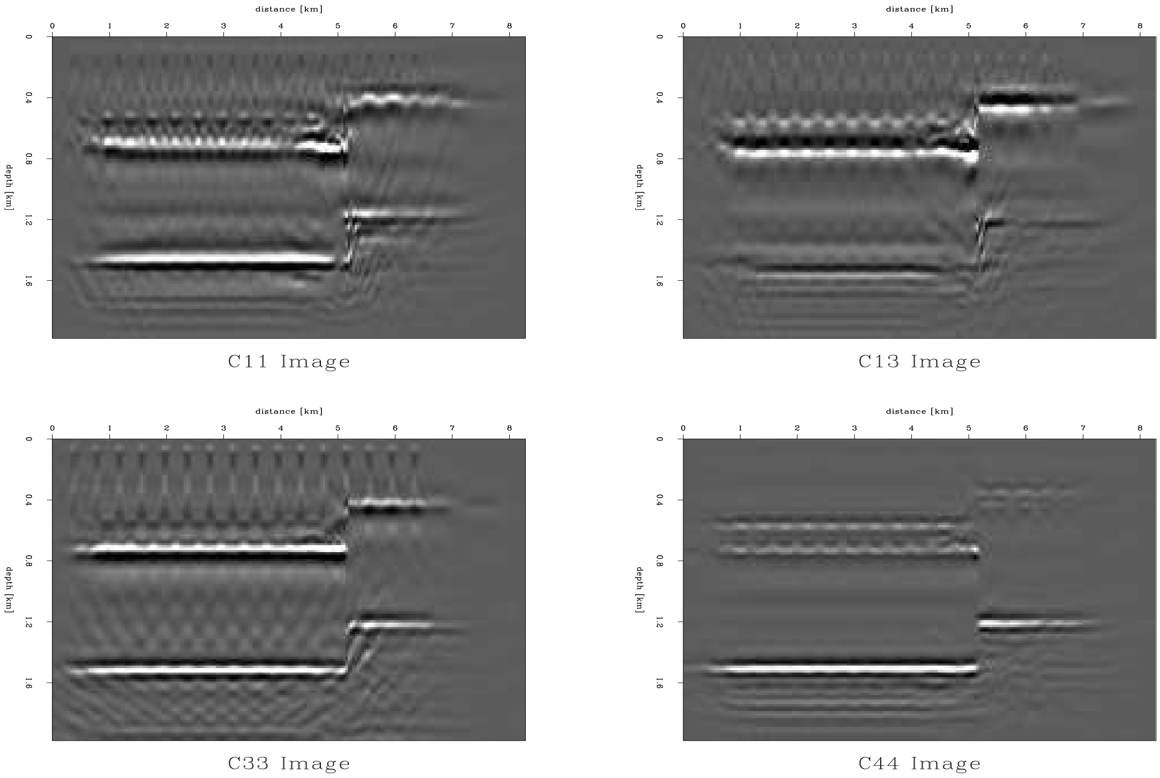

Figure 8: Elastic stiffnesses imaged using 16 shots. Source vector was vertical. martin3-ximagestack [NR]

without limitations in dip or ray paths. Massively parallel computers make feasable processing schemes that maintain correct amplitude information.

ACKNOWLEDGMENTS

Thanks to John Etgen whose modeling progams served as a starting point for the reverse time migration implementation. Also thanks to Biondo Biondi who always had time to discuss possible speed ups of the algorithm on the Connection Machine.

REFERENCES

Etgen, J., 1988, Finite difference elastic anisotropic wave propagation: SEP–**56**, 23–59.

Clayton, R., 1980, An inversion method for elastic wave fields: SEP–**24**, 81–92.

Mora, P., 1987, Elastic wavefield inversion: Ph.D. Thesis, Stanford University; also SEP–**52**.

Muir, F., A simplified canonical form for monoclinic systems: SEP–**70**.